

Synthesis and superconducting properties of niobium nitride nanowires and nanoribbons

U. Patel, S. Avci, Z. L. Xiao,^{a)} J. Hua, S. H. Yu, and Y. Ito
Department of Physics, Northern Illinois University, DeKalb, Illinois 60115, USA

R. Divan and L. E. Ocola
Center for Nanoscale Materials, Argonne National Laboratory, Argonne, Illinois 60439, USA

C. Zheng
Department of Chemistry and Biochemistry, Northern Illinois University, DeKalb, Illinois 60115, USA

H. Claus, J. Hiller, U. Welp, D. J. Miller, and W. K. Kwok
Materials Science Division, Argonne National Laboratory, Argonne, Illinois 60439, USA

(Received 12 July 2007; accepted 30 September 2007; published online 18 October 2007)

Superconducting niobium nitride wires and ribbons with transverse dimensions down to tens of nanometers were synthesized by annealing NbSe₃ nanostructure precursors in flowing ammonia gas at temperatures up to 1000 °C. Their critical temperatures increase with increasing annealing temperatures and reach 9–11.2 K when sintered at 950 °C or above. X-ray diffraction analyses identified Nb₄N₅ and Nb₅N₆ phases, dominating at annealing temperatures below and above 950 °C, respectively. Transport measurements show magnetoresistance oscillations at temperatures near the superconducting transition due to vortex-row confinement effects and voltage jumps in current-voltage characteristics at low temperatures attributed to hot-spot behavior. © 2007 American Institute of Physics. [DOI: 10.1063/1.2800809]

Freestanding superconducting nanowires and nanoribbons provide unique platforms for investigating superconductors in confined geometries, leading to scientific discoveries and applications. For example, superconducting nanowires with diameter comparable to the superconducting coherence length have served as a model system to study thermal and quantum phase slips.^{1–3} An “antiproximity effect” where bulk superconductors suppress the superconductivity of a nanowire was observed in superconducting Zn nanowires with Sn and In electrodes.⁴ A highly sensitive local magnetometer based on quantum interference effects and a superconducting phase gradiometer based on thermal phase slips can be fabricated from a pair of superconducting nanowires.⁵ Superconducting nanowires and nanoribbons with increased transverse dimensions are also interesting systems for exploring the properties of “few-row” vortex lattice where the sample edges play a crucial role in the arrangement and motion of vortices.^{6,7}

Recent advances in nanofabrication techniques have yielded a variety of superconducting nanowires, such as nanowires of Pb (Refs. 8–10) and Sn (Refs. 10 and 11) synthesized by electrodeposition into nanochannels of porous membranes and MoGe (Refs. 1 and 2) and Nb (Refs. 12) nanowires fabricated by sputtering the superconducting material onto bridges formed by suspended carbon nanotubes. Progress has also been made in synthesis of Pb nanowires by thermal decomposition of lead acetate in ethylene glycol¹³ and by electrodepositing Pb onto graphite electrodes at high reduction potentials.¹⁴ Recently, nanowires of two-band superconductor MgB₂ have also been fabricated by annealing B nanowires in Mg vapors^{15,16} and directly sintering MgBr₂ and NaBH₄ precursor gels in a controlled atmosphere of diborane and nitrogen.¹⁷ Finally, synthesis of NbSe₂ nano-

wires and nanoribbons has also been achieved using a conversion method based on controlled composition adjustment of NbSe₃ nanostructure precursors.¹⁸

Nitrides of niobium are well-known superconductors.¹⁹ Their relatively high critical temperatures and stability at ambient atmosphere have targeted them as potential candidates for applications in superconducting devices, such as single photon detectors^{20,21} and hot-electron bolometric mixers.^{22,23} For these applications, nano- or microstripes patterned out of films were typically utilized.^{20–23} In this letter, we report the synthesis of freestanding niobium nitride nanowires and nanoribbons. Their superconducting properties were characterized by magnetization and four-probe transport measurements. We observed an oscillation in the magnetic field dependence of the resistance and voltage jumps in the current-voltage characteristics of the niobium nitride nanowires/ribbons.

We developed a synthesis approach comprised of two steps: first, we synthesized one-dimensional (1D) nanostructures of NbSe₃ and, second, we converted NbSe₃ nanostructures into niobium nitrides by adjusting their composition while *maintaining* their 1D nanostructure shapes. NbSe₃ nanostructure precursors were synthesized by mixing stoichiometric quantities of high purity (>99.99%) niobium and selenium powders. More synthesis details can be found in Ref. 24. Two routes were pursued in the conversion process, (i) annealing the NbSe₃ nanostructures in a flowing ultrahigh purity (>99.999%) nitrogen gas with 4% hydrogen and (ii) annealing them in a flowing gas of 5% ammonia in helium. The first route, with annealing temperatures between 700 and 1000 °C produced white powders of Nb₂O₅ and yellow powders composed of various phases of niobium oxides. No superconductivity was observed down to 1.8 K. This is consistent with the fact that due to the strong N–N bond in a nitrogen molecule, the reaction between Nb and

^{a)}Electronic mail: xiao@anl.gov or zxiao@niu.edu

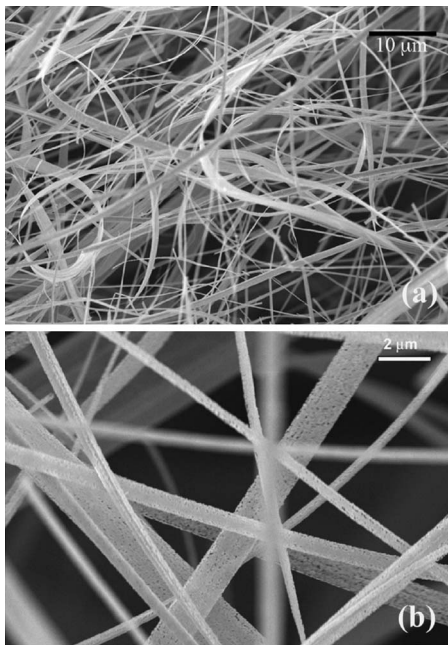


FIG. 1. SEM micrographs of superconducting niobium nitride nanowires and nanoribbons synthesized by annealing NbSe_3 nanostructure precursors in flowing ammonia gas at 950°C for 2 h. Images at low and high magnifications are presented in (a) and (b), respectively.

molecular nitrogen can only take place at temperatures above 1400°C ,^{25,26} and niobium is very reactive with oxygen. The second route, annealing the NbSe_3 nanostructures in flowing ammonia gas at 700 – 1000°C , resulted in a gray product which exhibited the presence of superconductivity.

The morphology of the precursors and final samples was analyzed with a scanning electron microscope (SEM) (Hitachi S-4700-II). Figure 1 shows SEM micrographs for the NbSe_3 nanostructures annealed at 950°C for 2 h. Wires and ribbons of various sizes can be seen. This size distribution of the annealed wires and ribbons follows that of the precursor NbSe_3 nanostructures which have transversal dimensions ranging from ~ 20 nm to a few micrometers and lengths up to millimeters.²⁴ Remarkably, the high annealing temperature (up to 1000°C) did not result in the collapse of the shape of the NbSe_3 nanostructures. It is possible that NbSe_3 first decomposes ($\text{NbSe}_3 \rightarrow \text{Nb} + \text{Se}$) and then Nb reacts with the ionic nitrogen to form niobium nitrides ($\text{Nb} + \text{NH}_3 \rightarrow \text{NbN}_x + \text{H}_2$). In fact, we noticed a red coloration of the exhaust line associated with selenium. A high magnification SEM micrograph shown in Fig. 1(b) reveals that the annealed wires and ribbons contain a high density of defects such as holes and gaps between grains, indicating their polycrystallinity.

We used powder x-ray diffraction (XRD) (Rigaku, model Miniflex, $\text{Cu K}\alpha$) to identify the phases of the synthesized materials. Figure 2 delineates the XRD patterns of the NbSe_3 nanostructures after annealing for 2 h at 765 , 840 , 910 , 950 , and 1000°C . No traces of the NbSe_3 phase are observed. All the diffraction peaks for the NbSe_3 nanostructures annealed at 765°C can be indexed to a Nb_4N_5 phase while peaks associated with a Nb_5N_6 phase appear in the XRD patterns for those annealed at 840°C and above.

A superconducting quantum interference device magnetometer was used to characterize the superconductivity of the converted niobium nitride nanostructures (in the amount of milligrams). The temperature dependence of the magnetization for the samples processed at the aforementioned anneal-

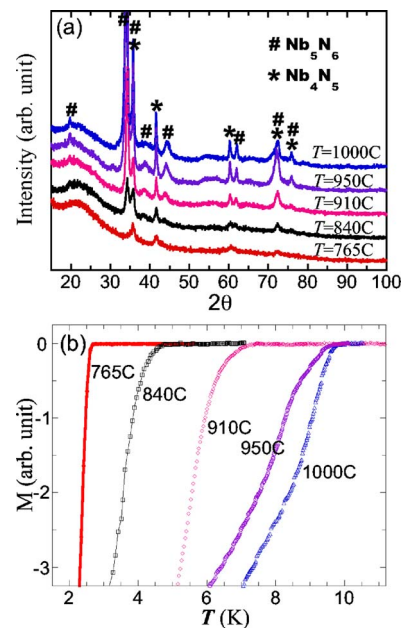


FIG. 2. (Color online) Structural and magnetization analyses of the niobium nitride nanostructures synthesized at various annealing temperatures. (a) Powder x-ray diffraction patterns and (b) magnetization vs temperature curves (measured at 0.1 G).

ing temperatures is presented in Fig. 2(b). The superconducting critical temperature (T_c) increases from ~ 2.5 to 9.7 K when the annealing temperature is raised from 765 to 1000°C . Furthermore, the superconducting transition becomes sharper for samples synthesized at lower temperatures. Interestingly, there are more than two distinct critical temperatures despite the fact that XRD analyses reveal only Nb_4N_5 and Nb_5N_6 phases. This can be understood from the fact that niobium nitrides are always nitrogen deficient and T_c is highly sensitive to slight changes in the crystalline lattice parameters.²⁵ From the XRD and magnetization data, we surmise that Nb_4N_5 represents the lower T_c (up to ~ 7 K) phase which dominates the samples sintered at 910°C and below, while the Nb_5N_6 phase has higher T_c and is the main component of the samples obtained at 950 and 1000°C .

Four-probe transport measurements were conducted to investigate the superconductivity of individual nanowires and nanoribbons. Electrical contacts were fabricated using photolithography and lift-off techniques. Figure 3(a) shows the temperature dependence of the resistance for three nanowires synthesized at 950°C . The resistance was normalized to their values at 14 K. The critical temperature (T_c), defined with a resistance criterion of $90\%R_N$, is 9.05 , 9.4 , and 11.2 K for samples A, B, and C, respectively. It indicates that the superconducting properties vary from wire to wire even under the same synthesis conditions. This variation cannot originate from the size effect since the diameters of all the three wires are a few hundred nanometers, which are much larger than the zero-temperature superconducting coherence length of niobium nitride, typically 3 – 5 nm.²⁷ It is most likely due to the slight difference in nitrogen stoichiometry among the different wires. In fact, the two-step superconducting transition found in samples A and C indicates that the nitrogen stoichiometry is probably inhomogeneous even within the same wire. This is consistent with the observation of two phases in the XRD pattern given in Fig. 2(a). We carried out further measurements on sample B which showed

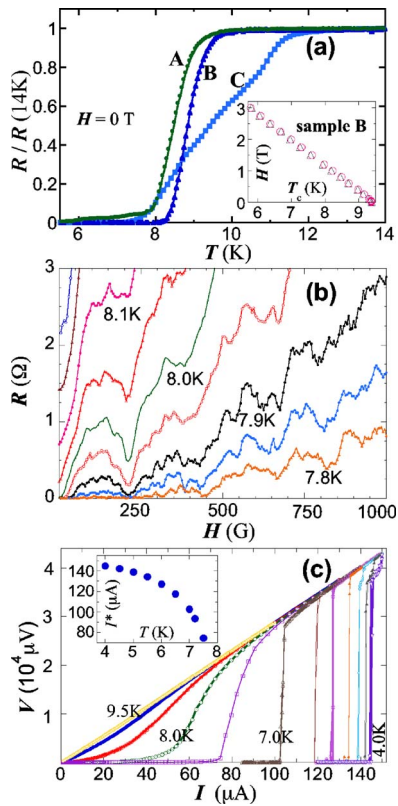


FIG. 3. (Color online) Four-probe transport measurements of individual niobium nitride nanowires measured with a current of $10 \mu\text{A}$. (a) Zero field R vs T curves of three nanowires (denoted samples A, B, and C). Inset to (a) contains H - T phase diagrams of sample B as prepared (open circles) and exposed to air for 3 weeks (open triangles). (b) and (c) are R - H curves at various fixed temperatures and zero-field I - V curves at various fixed temperatures for sample B, respectively. Inset to (c) presents the temperature dependence of the current I^* at which the voltage increases abruptly.

no apparent two-step transition to study the superconducting properties of the niobium nitride nanostructures. The diameter of sample B is ~ 650 nm and the superconducting transition width (temperature difference at 10% R_N and 90% R_N) is 0.9 K. The distance between voltage leads is $5 \mu\text{m}$.

The superconducting phase diagram, $H(T)$, for sample B obtained by measuring the resistance versus temperature curves in various magnetic fields with a current of $10 \mu\text{A}$ is shown in the inset of Fig. 3(a), where the applied magnetic field is perpendicular to the long axis of the wire. The superconducting coherence length of $\xi_0 = 6.5$ nm, determined from $dH_{c2}/dT = -0.82$ T/K, is consistent with typical values for niobium nitride.²⁷ In order to examine the stability of the wire in atmosphere, we remeasured sample B after leaving it exposed to air for 3 weeks. The superimposed phase diagrams [Fig. 3(a) inset, open circles and open triangles] indicate that its superconducting properties were not affected by the exposure to air.

As discussed in the introduction, superconducting nanowires and nanoribbons can be an ideal system to explore properties of few-row vortex lattice. In transport measurements, the critical current and resistance are predicted to oscillate with sweeping magnetic field which leads to a change in the number of rows and rearrangement of the vortex lattice. We find in sample B an oscillation in the resistance versus magnetic field curves obtained at temperatures close to T_c [Fig. 3(b)]. Furthermore, voltage jumps also appear in the I - V characteristics at low temperatures in sample B [Fig.

3(c)]. As shown in the inset of Fig. 3(c), $I^*(T)$ exhibits the typical parabolic form expected for hot-spot effect related to thermal heating.²⁸ Since the cross-sectional dimension of sample B is much larger than the superconducting coherence length, the phase slips observed in narrower superconducting nanowires should not occur in our sample at low temperatures. Thus, the hot spots in our samples are most likely caused by defects.

This material is based upon work supported by the U.S. Department of Energy, Award No. DE-FG02-06ER46334 and Contract No. DE-AC02-06CH11357. S.A. and Z.X. also acknowledge support from the National Science Foundation (NSF) under Award No. DMR-060762. SEM analysis and photolithography nanocontacting were performed at Argonne's Electron Microscopy Center (EMC) and Center for Nanomaterials (CNM), respectively.

¹A. Bezryadin, C. N. Lau, and M. Tinkham, *Nature (London)* **404**, 971 (2000).

²C. N. Lau, N. Markovic, M. Bockrath, A. Bezryadin, and M. Tinkham, *Phys. Rev. Lett.* **87**, 217003 (2001).

³M. L. Tian, J. G. Wang, J. S. Kurtz, Y. Liu, M. H. W. Chan, T. S. Mayer, and T. E. Mallouk, *Phys. Rev. B* **71**, 104521 (2005).

⁴M. Tian, N. Kumar, S. Xu, J. Wang, J. S. Kurtz, and M. H. W. Chan, *Phys. Rev. Lett.* **95**, 076802 (2005).

⁵D. S. Hopkins, D. Pekker, P. M. Goldbart, and A. Bezryadin, *Science* **308**, 1762 (2005).

⁶J. J. Palacios, *Phys. Rev. B* **57**, 10873 (1998).

⁷A. Falk, M. M. Deshmukh, A. L. Prieto, J. J. Urban, A. Jonas, and H. K. Park, *Phys. Rev. B* **75**, 020501 (2007).

⁸G. Yi and W. Schwarzacher, *Appl. Phys. Lett.* **74**, 1746 (1999).

⁹D. Y. Vodolazov, F. M. Peeters, L. Piraux, S. Matefi-Tempfli, and S. Michotte, *Phys. Rev. Lett.* **91**, 157001 (2003).

¹⁰S. Michotte, S. Matefi-Tempfli, and L. Piraux, *Appl. Phys. Lett.* **82**, 4119 (2003).

¹¹M. L. Tian, J. G. Wang, J. Snyder, J. Kurtz, Y. Liu, P. Schiffer, T. E. Mallouk, and M. H. W. Chan, *Appl. Phys. Lett.* **83**, 1620 (2003).

¹²A. Rogachev and A. Bezryadin, *Appl. Phys. Lett.* **83**, 512 (2003).

¹³Y. L. Wang, X. C. Jiang, T. Herricks, and Y. N. Xia, *J. Phys. Chem. B* **108**, 8631 (2004).

¹⁴Z. L. Xiao, C. Y. Han, W. K. Kwok, H. H. Wang, U. Welp, J. Wang, and G. W. Crabtree, *J. Am. Chem. Soc.* **126**, 2316 (2004).

¹⁵Y. Y. Wu, B. Messer, and P. D. Yang, *Adv. Mater. (Weinheim, Ger.)* **13**, 1487 (2001).

¹⁶Q. Yang, J. Sha, X. Y. Ma, Y. J. Ji, and D. R. Yang, *Supercond. Sci. Technol.* **17**, L31 (2004).

¹⁷M. Nath, and M. B. A. Parkinson, *Adv. Mater. (Weinheim, Ger.)* **18**, 2504 (2006).

¹⁸Y. S. Hor, U. Welp, Y. Ito, Z. L. Xiao, U. Patel, J. F. Mitchell, W. K. Kwok, and G. W. Crabtree, *Appl. Phys. Lett.* **87**, 142506 (2005).

¹⁹Y. G. Li and L. Gao, *J. Am. Ceram. Soc.* **86**, 1205 (2003).

²⁰A. Korneev, P. Kouminov, V. Matvienko, G. Chulkova, K. Smirnov, B. Voronov, G. N. Gol'tsman, M. Currie, W. Lo, K. Wilsner, J. Zhang, W. Slysz, A. Pearlman, A. Verevkin, and R. Sobolewski, *Appl. Phys. Lett.* **84**, 5338 (2004).

²¹A. J. Kerman, E. A. Dauler, W. E. Keicher, J. K. W. Yang, K. K. Berggren, G. Goltsman, and B. Voronov, *Appl. Phys. Lett.* **88**, 111116 (2006).

²²J. Kawamura, R. Blundell, C. E. Tong, G. Goltsman, E. Gershenzon, and B. Voronov, *J. Appl. Phys.* **80**, 4232 (1996).

²³M. Hajenius, J. J. A. Baselmans, J. R. Gao, T. M. Klapwijk, P. A. J. de Korte, B. Voronov, and G. Gol'tsman, *Supercond. Sci. Technol.* **17**, S224 (2004).

²⁴Y. S. Hor, Z. L. Xiao, U. Welp, Y. Ito, J. F. Mitchell, W. K. Kwok, and G. W. Crabtree, *Nano Lett.* **5**, 397 (2005).

²⁵M. Gurvitch, J. P. Remeika, J. M. Rowell, J. Geek, and W. P. Lowe, *IEEE Trans. Magn.* **21**, 509 (1985).

²⁶C. C. Agrafiotis, J. A. Puszynski, and V. Hlavacek, *J. Am. Ceram. Soc.* **74**, 2912 (1991).

²⁷T. Ohashi, H. Kitano, A. Maeda, H. Akaile, and A. Fujimaki, *Phys. Rev. B* **73**, 174522 (2006).

²⁸A. V. Gurevich, *Rev. Mod. Phys.* **59**, 941 (1987).